*2009*년 *2*월
석사학위논문

Residual Stress Prediction in Dissimilar Metals Welding Zones Using Data-based Modeling

조 선 대 학 교 대 학 원
원 자 력 공 학 과
임 동 혁

Residual Stress Prediction in Dissimilar Metals Welding Zones Using Data-based Modeling

- 데이터 기반 모델링 방법을 이용한
이종금속 용접부 잔류응력 예측 -

*2009*년 *2*월 *25*일

조 선 대 학 교 대 학 원

원 자 력 공 학 과

임 동 혁

Residual Stress Prediction in Dissimilar Metals Welding Zones Using Data-based Modeling

지도교수 나 만 균

이 논문을 공학 석사학위신청 논문으로 제출함.

*2008*년 *10*월

조 선 대 학 교 대 학 원

원 자 력 공 학 과

임 동 혁

임동혁의 석사학위 논문을 인준함

위원장　조선대학교　교수　송 종 순　(인)

위　원　조선대학교　교수　김 숭 평　(인)

위　원　조선대학교　교수　나 만 균　(인)

*2008*년　*11*월

조 선 대 학 교 대 학 원

CONTENTS

List of Tables

List of Figures

Abstract

Residual Stress Prediction in Dissimilar Metals Welding Zones Using Data-based Modeling

임 동 혁

지도 교수 : 나 만 균

조선대학교 일반대학원 원자력공학과

원자력 발전소 배관의 용접부 잔류 응력은 PWSCC (Primary Water Stress Corrosion Cracking)를 일으키는 중요한 요인이기 때문에 PWSCC를 예방하기 위해 잔류 응력을 정확히 예측하는 것은 아주 중요하다. 이렇듯 잔류 응력을 예측하기 위해 데이터를 기반으로 하는 많은 인공지능 모델들이 개발되었고 지금도 연구되고 있다.

본 논문에서는 몇몇의 데이터 기반 인공지능 모델 중 세 가지 모델 (Support Vector Regression, Fuzzy Support Vector Regression, Fuzzy Neural Network)을 잔류 응력 예측을 위해 사용하였으며, 각각의 방법론을 고찰하였다. 그리고 Subtractive Clustering Method와 Genetic 알고리즘을 사용함으로서 유용한 정보를 갖는 데이터를 얻고 제안된 알고리즘을 최적화시킬 수 있었다. 또한 성능 향상과 인공지능 방법의 잠재적인 Overfitting 문제를 해결하여 신뢰성 증진을 달성하기 위해 각각의 알고리즘을 적용했을 뿐만 아니라 서로 다른 모델을 결합함으로써 성능을 확인하였다.

예측성능을 비교해 본 결과 SVR 모델과 FSVR 모델 결과를 통합한 방법의 성능이 다른 방법의 결과에 비해 더 우수하다는 것을 알 수 있었으며, 이를 통해 실제 발전소 내에서 잔류 응력을 예측하기 위한 위 방법론이 적용가능하리라 기대된다.

Ⅰ. *Introduction*

The factors that have an effect on fatigue strength are residual stress, stress concentration, the mechanical properties of the material, and the macrostructure and microstructure. Among them, Residual stress is one of the most important factors and its effect on high-cycle fatigue is of more concern than the other factors. Residual stress is a tension or compression that exists in a material without external load being applied and the residual stresses in a component or structure are caused by incompatible internal permanent strains. And welding is one of the most significant causes of residual stresses and typically produces large tensile stresses. Welding joins the components of a structure together. On the other hand, the complex thermal cycles from welding result in formation of residual stresses in the joint region and distortion of the welded structure. Both welding residual stress and distortion can significantly impair the performance and reliability of the welded structures.

In particular, stress-corrosion cracking usually occurs when the following three factors exist at the same time: susceptible material, corrosive environment, and tensile stress (including residual stress). Thus, residual stress becomes very critical for stress-corrosion cracking when it is difficult to improve the material corrosivity of the components and their environment under operating conditions [1]. Since the welding residual stress is a major factor to generate Primary Water Stress Corrosion Cracking (PWSCC), it is important to predict the welding residual stress for preventing the PWSCC.

Residual stresses may be measured by non-destructive techniques and locally destructive techniques. The non-destructive techniques include X-ray and neutron diffraction methods, magnetic methods, and ultrasonic techniques and the locally destructive techniques includes hole drilling methods, the ring core techniques, and the sectioning methods.

In recent years, there has been a rapid increase in efforts to predict residual stresses by numerical modeling of welding processes. Modeling of welding is technically and computationally demanding, and simplification and idealization of the material behavior, process parameters and geometry is inevitable. Numerical modeling is a powerful tool for predicting residual stress. Over the past two decades, the finite element method has been used to predict residual stress due to welding. Simulations of welding processes involve thermo-mechanical finite element analyses (FEAs) of the welding zone [2].

In this thesis, a support vector regression (SVR), a fuzzy neural network (FNN), a fuzzy support vector regression (FSVR) model among the artificial intelligence methods which have been studied to develop data-based models are applied to easily evaluate the welding residual stress for weld zones of different kinds of metals. With training, these algorithms which are applied can be adept to exceptional nonlinear function approximation. And in order to optimize and test these models, the welding residual stress data should be acquired at first. These data were obtained in a previous work [3] by performing FEAs for various welding conditions such as pipeline shapes, welding heat input, welding metal strength, and the constraint of the pipeline end parts. Note that this thesis does not focus on the accuracy of FEA models for estimating the welding residual stress but focuses on the nonlinear prediction of the welding residual stress using these algorithms, based on the assumption that the FEA models are accurate.

Dissimilar welding joint between a nozzle and a pipe is regarded in the analyses since it has been known to be highly susceptible to PWSCC in the primary systems of nuclear power plants. Then, on the basis of the acquired data, SVR, FSVR and FNN models are developed to easily evaluate the residual stress in the welding of dissimilar metals for pipelines at NPPs. Also, the method combined with the different models has been used to solve the prospective overfitting problems of a performance improvement and accomplish the increase of reliability.

Ⅱ. *Computation of Welding Residual Stress Using FEA*

A. Analysis Conditions

Parametric FEAs had been carried out to obtain the data on welding residual stress under various welding conditions [3]. A dissimilar welding joint between a nozzle and a pipe is regarded in the analyses (see Fig. 1), because such joints are known to be highly susceptible to PWSCC in the primary systems of nuclear power plants. The base metals of the nozzle and the pipe were assumed to be SA508 ferritic steel and TP 316 austenite stainless steel, respectively, and Alloy 82/182 was used as a filler metal. Next, a ferritic steel nozzle was buttered with Alloy 82 and treated with heat after the welding. A gas tungsten arc weld was used with the Alloy 82 filler metal in the first pass welding for the root gap, and then a shielded metal arc weld was used with the Alloy 182 filler metal for the remaining passes.

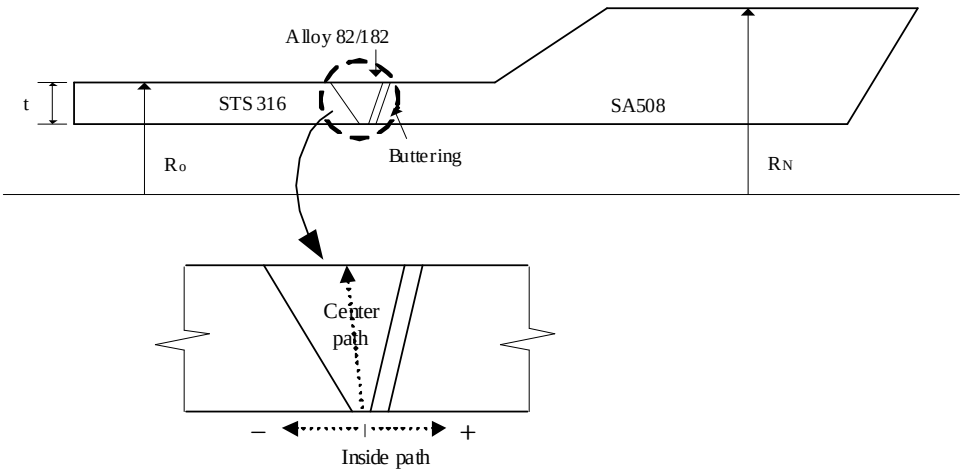

Fig. 1. A Welding Zone of Dissimilar Metals and Prediction Paths in the Welding Zone for Data Acquisition

The residual stress of a nozzle-pipe welding joint is usually affected by pipe thickness, heat input, the strength of welding metals, and the constraints of welded pipes. Therefore, a combination of these parameters was used as input data in the parametric FEA. Table 1 summarizes the values of each parameter and the constraint conditions of the pipes.

Table 1. Conditions for Analyzing Welding Residual Stress

Pipeline shape			Heat input, H [kJ/sec]	Yield stress of weld metal, σ_{ys} [MPa]	Constraint of end section
R_o[mm]	R_N[mm]	R_o/t	Pass 1; others		
205.6	300.10	4.8778	0.49764; 1.2690 0.55985; 1.4277	192.33 203.06	Restrained
205.6	271.75	6.8763	0.62205; 1.5863	213.70	
205.6	256.80	8.8735	0.68426; 1.7449 0.74646; 1.9036	224.38 235.07	
205.6	300.10	4.8778	0.49764; 1.2690 0.55985; 1.4277	192.33 203.06	Free
205.6	271.75	6.8763	0.62205; 1.5863	213.70	
205.6	256.80	8.8735	0.68426; 1.7449 0.74646; 1.9036	224.38 235.07	

B. Finite Element Models

The welding simulation of finite element analyses consists of a thermal analysis, which represents a thermal process during welding, followed by a structural analysis based on the results of the thermal analysis. Therefore, a sequentially coupled thermal-stress analysis was used to calculate the welding residual stress. For the structural analysis, the temperature contours was taken, which were made available by the thermal analysis, and they were used as input data to compute a range of stress contours. For these analyses, three types of axisymmetric

two-dimensional finite element models (as shown in Fig. 2) were developed, which vary in relation to the thickness of the pipes. Several studies have shown that an axisymmetric model is sufficient to simulate a pipe welding joint [4-6], even though real welding is a three-dimensional procedure.

To calculate the welding residual stress, the ABAQUS program was used to perform the coupled FEAs [7]. Also, an 8-node quadratic quadrilateral axisymmetric diffusive heat transfer (DCAX8 in ABAQUS) was used as a finite element in the thermal analysis; in addition, an 8-node biquadratic axisymmetric stress/displacement quadrilateral with reduced integration (CAX8R in ABAQUS) was used as the element in the structural analysis.

The welding process was simulated by eight welding passes for $R_o/t = 8.8735$, nine welding passes for $R_o/t = 6.8763$, and 11 welding passes for $R_o/t = 4.8778$. Each bead in the model was considered to be a pass so that the number of passes in the finite element model was equal to the number of beads in the simulated welding. In the meshing, each pass was identified by grouping the corresponding elements and activating them incrementally to simulate the deposit of each bead. Given the assumption that post-welding heat treatment is conducted after the buttering, the buttering procedure in the models was ignored. Also, the metallurgical transformations in the ferritic steel was ignored; that is, in the heat-affected zone and with respect to the dilution between the base and welding metals. However, the annealing effect was considered in the models, and the annealing temperature was 1400℃.

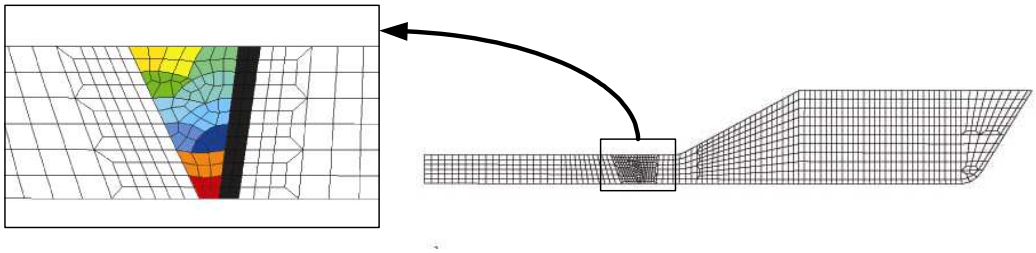

(a) $R_o/t = 4.8778$

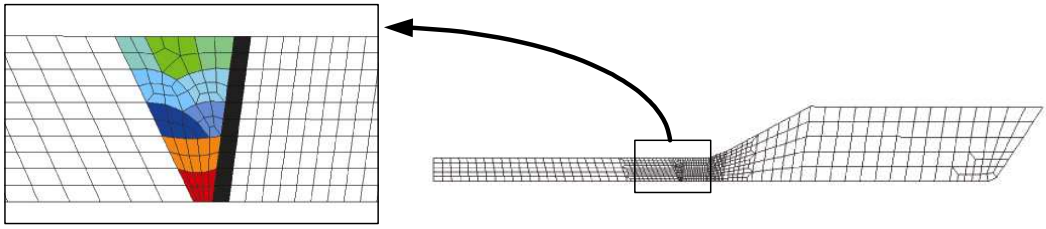

(b) $R_o/t = 6.8763$

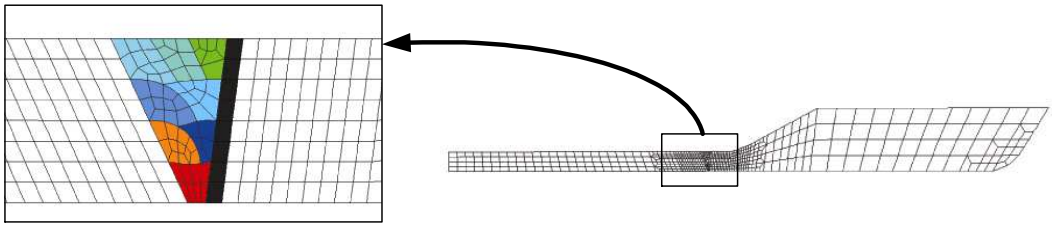

(c) $R_o/t = 8.8735$

Fig. 2. Axisymmetric Finite Element Models for a Nozzle-pipe Dissimilar Metal Weld Joint

Ⅲ. *Data-based Models to Predict Welding Residual Stress*

A. Support Vector Regression (SVR)

An SVR method was presented in the previous work [8] to estimate the residual stress for dissimilar metal welding in accordance with various welding conditions. The estimation of continual variables is known as regression. The classical regression techniques are based on the strict assumption that probability distribution functions are known. Regrettably, in a lot of practical situations, there is not enough information about the underlying probability distribution laws. For the most part, all we have are recorded training patterns which are usually high dimensional. Therefore, probability distribution-free regression techniques are required that do not need knowledge of probability distributions. Recently, learning and soft computing-based approaches such as neural networks (NNs) and SVRs have widely been used in functional regression problems [9-12]. Although both data modeling methods of NNs and SVRs show comparable results on the most popular benchmark problems, the theoretical status of SVRs makes them an attractive and promising area of research [13].

The SVR is to map nonlinearly the original data $\boldsymbol{x}$ into a higher-dimensional feature space. That is, in order to learn nonlinear relations with a linear machine, it is required to select a set of nonlinear feature and to express the data in the new representation. This transformation can be achieved by using various nonlinear mapping. Nonlinear regression problems in input space can become linear regression problems in feature space.

The SVR model is given N training data $\{(\boldsymbol{x}_i, y_i)\}_{i=1}^{N} \in R^m \times R$ where $\boldsymbol{x}_i$ is the

input vector to the SVR model and y_i is the actual output value, from which it learns the input-output relationship. The SVR model can be expressed as follow [13]:

$$y = f(\boldsymbol{x}) = \sum_{i=1}^{N} w_i \phi_i(\boldsymbol{x}) + b = \boldsymbol{w}^T \boldsymbol{\phi}(\boldsymbol{x}) + b \tag{1}$$

where the function $\phi_i(\boldsymbol{x})$ is called the feature that is nonlinearly mapped from the input space $\boldsymbol{x}$, $\boldsymbol{w} = [w_1\ w_2\ \cdots\ w_N]^T$, and $\boldsymbol{\phi} = [\phi_1\ \phi_2\ \cdots\ \phi_N]^T$.

Eq. (1) is a nonlinear regression model because the resulting hyper-surface is a nonlinear surface hanging over the m-dimensional input space. However, after the input vectors $\boldsymbol{x}$ are mapped into vectors $\boldsymbol{\phi}(\boldsymbol{x})$ of a high dimensional kernel-induced feature space, the nonlinear regression model is turned into a linear regression model in this feature space. The nonlinear function is learned by a linear learning machine where the learning algorithm minimizes a convex functional. The convex functional is expressed as the following regularized risk function, and the parameters $\boldsymbol{w}$ and b are a support vector weight and a bias that are calculated by minimizing the risk function:

$$R(\boldsymbol{w}) = \frac{1}{2}\boldsymbol{w}^T\boldsymbol{w} + \lambda \sum_{i=1}^{N} |y_i - f(\boldsymbol{x})|_\epsilon \tag{2}$$

where

$$|y_i - f(\boldsymbol{x})|_\epsilon = \begin{cases} 0 & |y_i - f(\boldsymbol{x})| < \epsilon \\ |y_i - f(\boldsymbol{x})| - \epsilon & otherwise \end{cases} \tag{3}$$

The constant λ is called a regularization parameter. The regularization parameter determines the trade-off between the approximation error and the weight vector norm. An increase of the regularization parameter λ penalizes larger errors, which leads to a decrease of approximation error. This can also be achieved easily by increasing the weight vector norm. However, an increase in the weight vector norm does not make sure of the good generalization of the SVR model. The constants λ and ϵ are user-specified parameters and $|y_i - f(\boldsymbol{x})|_\epsilon$ is called the ϵ-insensitive loss function [14]. The loss equals zero if the predicted value $f(\boldsymbol{x})$ is

within an error level ϵ, and for all other predicted points outside the error level ϵ, the loss is equal to the magnitude of the difference between the predicted value and the error level ϵ (refer to Figs. 3 and 4).

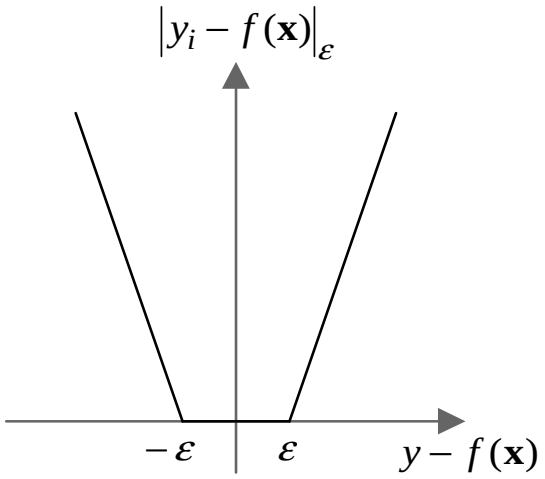

Fig. 3. Linear ϵ-insensitive Loss Function.

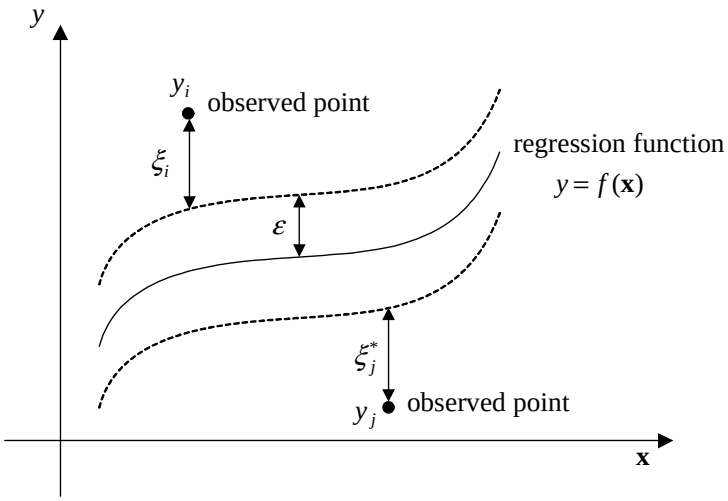

Fig. 4. Insensitive ϵ-tube and Slack Variables ξ_i and ξ_j^* for the SVR Model.

Increasing the insensitivity zone ϵ means a reduction in requirements for the accuracy of approximation and it also decreases the number of support vectors, leading to data compression. In addition, increasing the insensitivity zone ϵ has smoothing effects on modeling highly noisy polluted data. The foregoing regularized risk function is converted into the following constrained risk function:

$$R(\boldsymbol{w},\xi,\xi^*) = \frac{1}{2}\boldsymbol{w}^T\boldsymbol{w} + \lambda\sum_{i=1}^{N}(\xi_i+\xi_i^*) \tag{4}$$

subject to the constraints

$$\begin{cases} y_i - \boldsymbol{w}^T\boldsymbol{\phi}(\boldsymbol{x}) - b \le \epsilon + \xi_i, & i = 1,2,\cdots,N \\ \boldsymbol{w}^T\boldsymbol{\phi}(\boldsymbol{x}) + b - y_i \le \epsilon + \xi_i^*, & i = 1,2,\cdots,N \\ \xi_i,\ \xi_i^* \ge 0, & i = 1,2,\cdots,N \end{cases} \tag{5}$$

where

$$\boldsymbol{\xi} = [\xi_1 \ \ \xi_2 \ \ \cdots \ \ \xi_N]^T,$$

$$\boldsymbol{\xi}^* = [\xi_1^* \ \ \xi_2^* \ \ \cdots \ \ \xi_N^*]^T.$$

The parameter ξ_i and ξ_i^* are slack variables representing upper and lower constraints on the outputs of the system, respectively, and they are positive values (refer to Fig. 4). The constrained optimization problem of Eq. (4) can be solved by applying the Lagrange multiplier technique to Eqs. (4) and (5) and then by using a standard quadratic programming techinque. Finally, the regression function of Eq. (1) becomes

$$y = f(\boldsymbol{x}) = \sum_{i=1}^{N}(\alpha_i - \alpha_i^*)K(\boldsymbol{x},\boldsymbol{x}_i) + b \tag{6}$$

where $K(\boldsymbol{x}_i,\boldsymbol{x}) = \boldsymbol{\phi}^T(\boldsymbol{x}_i)\boldsymbol{\phi}(\boldsymbol{x})$ is called the kernel function. A number of coefficients $\alpha_i - \alpha_i^*$ have nonzero values and the corresponding training data points are called support vectors and have approximation errors equal to or larger than ϵ.

B. Fuzzy Support Vector Regression (FSVR)

The FSVR is known as support vector regression (SVR) that is combined with a fuzzy concept. The proposed FSVR improves the SVR by reducing the effect of outliers and noise. By applying a fuzzy membership function to each data point of the SVR model, the regularized risk function can be reformulated, such that different input data points can make different contributions to the learning of a regression function as follows:

$$R(\boldsymbol{w}) = \frac{1}{2}\boldsymbol{w}^{\boldsymbol{T}}\boldsymbol{w} + \lambda\sum_{i=1}^{N}\mu_i|y_i - f(\boldsymbol{x})|_{\epsilon}, \tag{7}$$

where μ_i is a fuzzy membership grade. Commonly used SVR methods apply an equal weighting to all data points. However, FSVR uses different weightings according to their importance, which is specified by the fuzzy membership grade. Minimizing the regularized risk function is equivalent to minimizing the following constrained risk function:

$$R(\boldsymbol{w},\xi,\xi^*) = \frac{1}{2}\boldsymbol{w}^{T}\boldsymbol{w} + \lambda\sum_{i=1}^{N}\mu_i(\xi_i + \xi_i^*), \tag{8}$$

subject to the constraints

$$\begin{cases} y_i - \boldsymbol{w}^T\boldsymbol{\phi}(\boldsymbol{x}) - b \le \epsilon + \xi_i, & i = 1,2,\cdots,N \\ \boldsymbol{w}^T\boldsymbol{\phi}(\boldsymbol{x}) + b - y_i \le \epsilon + \xi_{i,}^*, & i = 1,2,\cdots,N \\ \xi_i,\ \xi_i^* \ge 0, & i = 1,2,\cdots,N \end{cases} \tag{9}$$

where the constant λ determines the trade-off between the complexity of $f(\boldsymbol{x})$ and the amount up to which deviations greater than ϵ are tolerated. The parameters $\boldsymbol{\xi} = [\xi_1\ \ \xi_2\ \cdots\ \xi_N]^T$ and $\boldsymbol{\xi}^* = [\xi_1^*\ \ \xi_2^*\ \cdots\ \xi_N^*]^T$ are the slack variables (which are positive) that represent the upper and lower constraints on the outputs of the system like an SVR.

The constrained optimization problem can be solved by applying the Lagrange multiplier technique to Eqs. (8) and (9), which is expressed by the following

Lagrange functional:

$$\Phi(\boldsymbol{w},b,\xi_i,\xi_i^*,\alpha_i,\alpha_i^*,\beta_i,\beta_i^*) = \frac{1}{2}\boldsymbol{w}^T\boldsymbol{w} + \lambda\sum_{i=1}^{N}\mu_i(\xi_i+\xi_i^*) - \sum_{i=1}^{N}\alpha_i\left[\boldsymbol{w}^T\boldsymbol{\phi}(\boldsymbol{x}_i)+b-y_i+\epsilon+\xi_i\right] \quad (10)$$
$$-\sum_{i=1}^{N}\alpha_i^*\left[y_i-\boldsymbol{w}^T\boldsymbol{\phi}(\boldsymbol{x}_i)-b+\epsilon+\xi_i^*\right] - \sum_{i=1}^{N}(\beta_i\xi_i+\beta_i^*\xi_i^*).$$

Minimizing Eq. (10) with respect to the primal variables, $\boldsymbol{w}, b, \xi_i, \xi_i^*$, gives the following conditions:

$$\boldsymbol{w} = \sum_{i=1}^{N}(\alpha_i-\alpha_i^*)\boldsymbol{\phi}(\boldsymbol{x}_i),$$

$$\sum_{i=1}^{N}(\alpha_i-\alpha_i^*) = 0,$$

$$\mu_i\lambda-\alpha_i-\beta_i = 0,\ \ i=1,2,\cdots,N,$$

$$\mu_i\lambda-\alpha_i^*-\beta_i^* = 0,\ \ i=1,2,\cdots,N.$$

The Lagrange functional [15] can be rewritten using the above minimum conditions as follows:

$$\Phi(\alpha_i,\alpha_i^*) = \sum_{i=1}^{N}y_i(\alpha_i-\alpha_i^*) - \epsilon\sum_{i=1}^{N}(\alpha_i+\alpha_i^*) - \frac{1}{2}\sum_{i=1}^{N}\sum_{l=1}^{N}(\alpha_i-\alpha_i^*)(\alpha_l-\alpha_l^*)\boldsymbol{\phi}^T(\boldsymbol{x}_i)\boldsymbol{\phi}(\boldsymbol{x}_l) \quad (11)$$

subject to the constraints

$$\begin{cases} \sum_{k=1}^{N}(\alpha_k-\alpha_k^*) = 0 \\ 0 \le \alpha_k \le \mu_k\lambda, \quad k=1,2,\cdots,N \\ 0 \le \alpha_k^* \le \mu_k\lambda, \quad k=1,2,\cdots,N \end{cases}$$

The above Lagrange functional can be solved by determining the values for α_i and α_i^* using a quadratic programming technique. Finally, the regression function of Eq. (1) is expressed as follows:

$$y = f(\boldsymbol{x}) = \sum_{i=1}^{N}(\alpha_i-\alpha_i^*)\boldsymbol{\phi}^T(\boldsymbol{x_i})\boldsymbol{\phi}(\boldsymbol{x}) + b = \sum_{i=1}^{N}(\alpha_i-\alpha_i^*)K(\boldsymbol{x},\boldsymbol{x}_i) + b, \quad (12)$$

where $K(\boldsymbol{x},\boldsymbol{x}_i) = \boldsymbol{\phi}^T(\boldsymbol{x}_i)\boldsymbol{\phi}(\boldsymbol{x})$ is known as the kernel function which is mentioned in

the section Ⅲ.A. The bias b is calculated as [14]

$$b = -\frac{1}{2}\sum_{i=1}^{N}(\alpha_i - \alpha_i^*)(K(\boldsymbol{x}_r, \boldsymbol{x}_i) + K(\boldsymbol{x}_s, \boldsymbol{x}_i)),$$

where $\boldsymbol{x}_r$ and $\boldsymbol{x}_s$ are support vectors and they are data points positioned at the boundary of the ϵ-insensitivity zone (refer to Fig. 4).

The four most relevant design parameters for the FSVR model are the insensitivity zone (ϵ), the regularization parameter (λ), the kernel function parameter (σ), and the fuzzy membership grade (μ). An increase in the insensitivity zone (ϵ), reduces the requirements for the accuracy of approximation and allows a decrease in the number of SVs, leading to data compression. In addition, increasing the insensitivity zone (ϵ) has smoothing effects on modeling highly noisy polluted data. An increase in the regularization parameter (λ), reduces larger errors, which lead to a decrease in the approximation error. This can also be achieved by increasing the weight vector norm. However, an increase in the weight vector norm decreases the good generalization capability of the FSVR model. The kernel function parameter (σ) determines the sharpness of the radial basis kernel function. The fuzzy membership grade will be explained in the section Ⅳ.B.

C. Fuzzy Neural Network (FNN)

In fuzzy inference modeling, it is relatively easy to set up rough fuzzy rules for a target system by intuition if we understand its dynamics well. However, the task of fine-tuning the fuzzy rules to improve modeling performance is difficult. Therefore, an FNN that can embody fuzzy inference models was proposed [3]. The proposed FNN provides functions for performing fuzzy inference. The functions can also be used to tune the parameters with respect to the shape of antecedent linguistic terms and the relative importance of rules.

A fuzzy inference model consists of situation and action pairs where conditional rules described in 'if-then statements' are generally used. The task of adapting fuzzy systems for on-line application involves neuronal improvements of fuzzy inference systems and the fuzzification of neural network systems. In this way we can exploit the complementary nature of fuzzy inference systems and neural network systems. The combination of the two systems is usually called an FNN system.

The fuzzy inference model can be accomplished through a clustering of numerical data. A cluster center is in essence a prototypical data point that exemplifies a characteristic behavior of a target system, and each cluster center can be used as the basis of a fuzzy rule that describes the system behavior. The development of a complete fuzzy system identification algorithm can therefore be based on the results of a subtractive clustering (SC) technique (This method will be explained in next chapter); this type of technique can be used as the basis of a fast and robust algorithm for identifying a fuzzy inference model [16]. Therefore, a fuzzy inference model based on an SC method can be used to predict the residual stress of dissimilar metal welding.

The data-based fuzzy inference model assumes the availability of N input/output training data pairs $(\boldsymbol{x}^T(k), y(k))$, where $\boldsymbol{x}^T(k) = (x_1(k), x_2(k), \cdots, x_m(k))$, $k = 1, 2, \cdots, N$. If we assume that the data points have been normalized in each dimension, the method can begin by generating a number of clusters in the $m \times N$ dimensional input space. To develop a systematic approach to the generation of fuzzy rules from a given input-output data set, we can use a Takagi-Sugeno-type fuzzy inference model [17], where the i-th fuzzy rule for the k-th time instant data is formulated as follows:

$$\begin{aligned} &If \;\; x_1(k) \;\; is \;\; A_{i,1}(k) \;\; AND \;\; \cdots \;\; AND \;\; x_m(k) \;\; is \;\; A_{i,m}(k), \\ &then \;\; \hat{y}_i(k) \;\; is \;\; f_i(x_1(k), \cdots, x_m(k)) \end{aligned} \tag{13}$$

where $x_j(k)$ is the input linguistic variable to the fuzzy inference model ($j = 1, 2, \cdots, m$; m= the number of input variables), $A_{i,j}(k)$ is the membership

function of the j-th input variable for the i-th fuzzy rule ($i = 1, 2, \cdots, n$; n= the number of rules), and $\hat{y_i}(k)$ is the output of the i-th fuzzy rule.

The SC method is applied to obtain the informative training data. And when the cluster estimation method is applied to a collection of input/output data, we can generate a number of n Takagi-Sugeno-type fuzzy rules, where the premise parts are fuzzy sets defined by the cluster centers that are obtained by the SC algorithm. The membership function value, $A_i(\boldsymbol{x}(k))$, of an input data vector, $\boldsymbol{x}(k)$, to the i-th cluster center,$\boldsymbol{x}_c(i)$, can be defined as follows:

$$A_i(\boldsymbol{x}(k)) = e^{-4\| \boldsymbol{x}(k) - \boldsymbol{x}_c(i) \|^2 / r_a^2}. \tag{14}$$

The fuzzy inference model output, $\hat{y_i}(k)$, is calculated by the weighted average of the consequent parts of the fuzzy rules as follows:

$$\hat{y}(k) \frac{\sum_{i=1}^{n} A_i(\boldsymbol{x}(k)) f_i(\boldsymbol{x}(k))}{\sum_{i=1}^{n} A_i(\boldsymbol{x}(k))}. \tag{15}$$

The function $f_i(\boldsymbol{x}(k))$ is a polynomial in the input variables, but it can be any function as long as it can appropriately describe the output of the fuzzy inference system within the fuzzy region specified by the antecedent of the rule. In the Takagi-Sugeno-type fuzzy inference model, the output of an arbitrary i-th fuzzy rule, f_i, is usually represented by the following first-order polynomial of inputs:

$$f_i(\boldsymbol{x}(k)) = \sum_{j=1}^{m} q_{ij} x_j(k) + r_i, \tag{16}$$

where q_{ij} is a weighting value of the j-th input on the i-th fuzzy rule output and r_i is a bias of the i-th fuzzy rule output.

The output of the fuzzy inference model given by Eq. (15) can therefore be rewritten as

$$\hat{y}(k) = \sum_{i=1}^{n} \overline{w_i} f_i(\boldsymbol{x}(k)) = \boldsymbol{w}^T(k) \boldsymbol{q}, \tag{17}$$

where

$$\overline{w_i}(k) = \frac{A_i(\boldsymbol{x}(k))}{\sum_{i=1}^{n} A_i(\boldsymbol{x}(k))},$$

$\boldsymbol{q} = [q_{1,1} \cdots q_{n,1} \cdots\cdots q_{1,m} \cdots q_{n,m}\ r_1 \cdots r_n]^T$, and

$\boldsymbol{w}(k) = [\overline{w_1}(k)x_1(k) \cdots \overline{w_n}(k)x_1(k) \cdots\cdots \overline{w_1}(k)x_m(k) \cdots \overline{w_n}(k)x_m(k)\ \ \overline{w_1}(k) \cdots \overline{w_n}(k)]^T$, $k = 1,2,\cdots, N$.

The value $\overline{w}_i(k)$ represents the normalized compatibility grade of the i-th fuzzy rule and consists of the input data and the normalized membership function values. The vector $\boldsymbol{q}$ is called the consequent parameter vector. Figure 5 describes the calculation procedure of the FNN model.

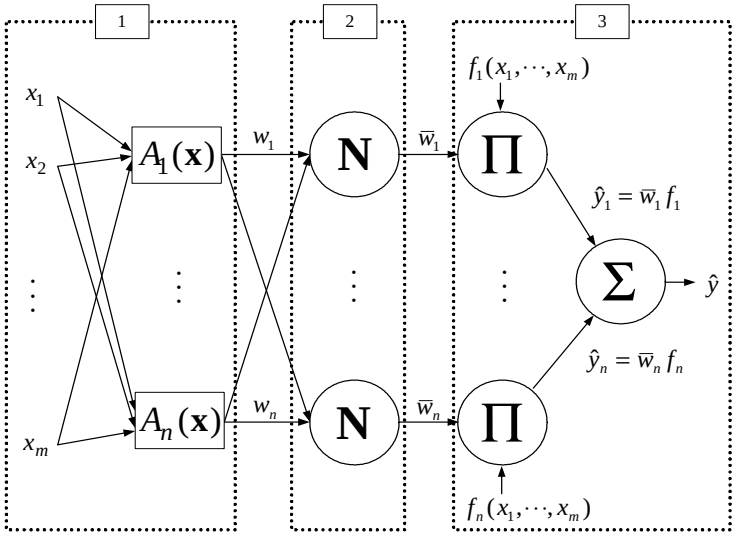

Fig. 5. A Fuzzy Neural Network Model

Ⅳ. *Optimization of Data-based Models and Selection of Training Data*

A. Optimization of Data-based Models

The SVR, FSVR and FNN models are designed by learning from given data and should be optimized to maximize the prediction performance. The performance of the SVR model depends heavily on the three kinds of design parameters such as the insensitivity zone ϵ, the regularization parameter λ, and the kernel function parameters. (In case of FSVR, four parameters (ϵ, λ, σ, μ) are considered.) Therefore, these parameters except for the fuzzy membership grade must be optimized by a genetic algorithm in order to maximize the performance of the SVR, FSVR and FNN models. If these parameters are not optimized, the three models can be inferior in performance.

Genetic algorithm is less susceptible to being stuck at local minima than conventional search methods since genetic algorithms start from many points simultaneously climbing many peaks in parallel. Also, the genetic algorithm is the most useful method to solve optimization problems with multiple objectives. The genetic algorithm is used to optimize the insensitivity zone ϵ, the regularization parameter λ, and the sharpness σ of the radial basis kernel function used in this thesis that is expressed as follow:

$$K(\boldsymbol{x}_i,\boldsymbol{x}) = \exp\left(-\frac{(\boldsymbol{x}-\boldsymbol{x}_i)^T(\boldsymbol{x}-\boldsymbol{x}_i)}{2\sigma^2}\right). \tag{18}$$

The genetic algorithm requires a fitness function that assigns a score to each chromosome (candidate solution) in the current population, and maximizes the fitness function value. The fitness function evaluates the extent to which each candidate solution is suitable for specified objectives. A root mean square (RMS)

error and a maximum error can be a measure of the prediction performance of the SVR, FSVR and FNN models. However, the minimization of the errors only may induce the overfitting in these models, which means that these models is fitted well for only a specific data set (training data) but is not fitted for another data set.

In usual learning problems, the proposed model is trained using exemplary situations (training data) for which the desired output is already known. It is assumed that the model will also be able to predict the correct output for other situations, thus generalizing to situations not presented during training. But especially in cases where learning was performed too long or where training data are rare, the proposed model may adjust to very specific random features of the training data, which have no causal relation to the target function. In this process of overfitting, the performance on the training data still increases while the performance on the test data becomes worse.

Regularization has been applied successfully to numerous machine learning problems including the avoidance of overfitting [18]. It is a well-known method for the treatment of mathematically ill-posed problems. In this thesis, through the regularization that these models are optimized independently by using a data set independent of the training data, this kind of overfitting problems can be overcome. Therefore, the acquired data are divided into three kinds of data sets such as the training data, the optimization data, and the test data. The training data are used to solve the coefficients $\alpha_i - \alpha_i^*$ and the bias b in Eq. (6) of the SVR and FSVR models.

In case of FNN, the training data are used to solve the antecedent parameters of the FNN model. The optimization data are used in optimizing the SVR, FSVR and FNN models by using another independent data set to improve generalization capability of these models. The test data are used to independently verify the developed these models. The specified multiple objectives are to minimize the RMS error along with the small maximum error:

$$F = \exp(-\mu_1 E_1 - \mu_2 E_2 - \mu_3 E_3 - \mu_4 E_4) \tag{19}$$

where μ_1, μ_2, μ_3 and μ_4 are the weighting coefficients. E_1 and E_2 indicate the root mean squared error for the training data and the optimization data, respectively. E_3 and E_4 indicate the maximum error for the training data and the optimization data. These parameters are defined as follows:

$$E_1 = \sqrt{\frac{1}{N_t}\sum_{i=1}^{N_t}(y_i^t - \hat{y}_i^t)^2}\,, \tag{20}$$

$$E_2 = \sqrt{\frac{1}{N_o}\sum_{i=1}^{N_o}(y_i^o - \hat{y}_i^o)^2}\,, \tag{21}$$

$$E_3 = \max\left\{y_i^t - \hat{y}_i^t\right\}, \tag{22}$$

$$E_4 = \max\left\{y_i^o - \hat{y}_i^o\right\}. \tag{23}$$

The variables y_i and $\hat{y_i}$ denote the measured output and the output predicted by the SVR, FSVR and FNN models, respectively. The number N represents the number of the training data. The superscripts, t and o, indicate the training data and the optimization data, respectively, and N_t and N_o represent the numbers of the training data and the optimization data.

In the FNN case, if the antecedent parameters are fixed by the genetic algorithm, the output of the resulting FNN model can be described as a series of expansions of some basis functions. The basis function expansion is linear in its adjustable parameters, as shown in Eq. (17), because $\boldsymbol{w}^T(k)$ is known by the genetic algorithm. Thus, we can use the least squares method to determine the consequent parameters. The consequent parameter $\boldsymbol{q}$ was chosen to minimize the following cost function, including the squared error between the target output $\boldsymbol{y}$ and the estimated output $\hat{\boldsymbol{y}}$:

$$J = \sum_{k=1}^{N_t}(y(k) - \hat{y}(k))^2 = \sum_{k=1}^{N_t}(y(k) - \boldsymbol{w}^T(k)\boldsymbol{q})^2 = \frac{1}{2}(\boldsymbol{y} - \hat{\boldsymbol{y}})^2, \tag{24}$$

where

$\boldsymbol{y} = [y(1)\ y(2) \cdots\ y(N_t)]^T$ and $\hat{\boldsymbol{y}} = [\hat{y}(1)\ \hat{y}(2) \cdots\ \hat{y}(N_t)]^T$.

The solution for minimizing the above cost function can be obtained by

$$\boldsymbol{y} = \hat{\boldsymbol{y}} = \boldsymbol{W}\boldsymbol{q}, \tag{25}$$

where

$$\boldsymbol{W} = [\boldsymbol{w}(1)\ \boldsymbol{w}(2) \cdots\ \boldsymbol{w}(N_t)]^T .$$

To solve the parameter vector $\boldsymbol{q}$ in Eq. (25), we should ensure that the matrix $\boldsymbol{W}$ is invertible but not usually a square matrix. We can easily solve the parameter vector $\boldsymbol{q}$ in Eq. (25) by using the pseudo-inverse of the $\boldsymbol{W}$ matrix as follows:

$$\boldsymbol{q} = (\boldsymbol{W}^T\boldsymbol{W})^{-1}\boldsymbol{W}^T\boldsymbol{y}. \tag{26}$$

The parameter vector $\boldsymbol{q}$ can be calculated with a series of N_t input/output data pairs prepared for the training data.

B. Selection of Training Data

To increase the learning efficiency, the three models should be trained well by using informative data. It is expected that input and output training data have a lot of clusters and the data at these cluster centers is more informative than neighboring data. Figure 6 shows data clusters and their centers (indicated as '+' signs) for simple two-dimensional data.

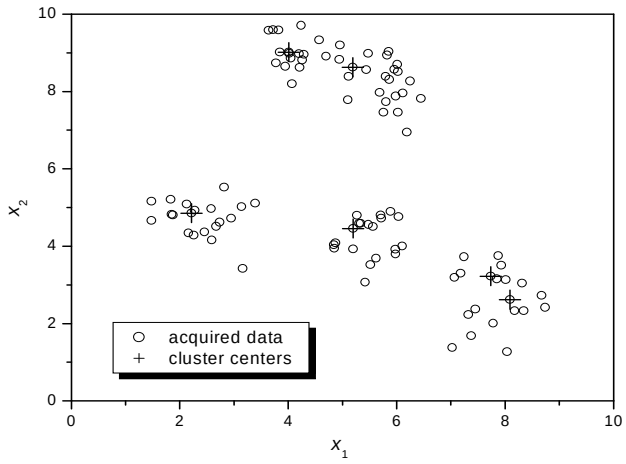

Fig. 6. Data Clusters and Cluster Centers for Simple Two-dimensional Data.

In this thesis, the cluster centers are found out by a subtractive clustering (SC) scheme [16]. The SC scheme assumes the availability of N input/output training data $\boldsymbol{z}_i = (\boldsymbol{x}_i, y_i)$, $i = 1,2,...,N$, and also, it is assumed that the data points have been normalized in each dimension. The scheme starts by generating a number of clusters in the m-dimensional input space. The SC scheme considers each data point as a potential cluster center and uses a measure of the potential of each data point, which is defined as a function of the Euclidean distances to all other input data points [16]:

$$P_1(i) = \sum_{j=1}^{N} e^{-4\|\boldsymbol{x}_i - \boldsymbol{x}_j\|^2 / r_\alpha^2}, \; i = 1,2,\cdots,N, \tag{27}$$

where r_α is a radius, defining a neighborhood, which has considerable influence on the potential. Obviously, the potential of a data point is high when it is surrounded by many neighboring data. After the potential of every data point has been computed, the data point with the highest potential is selected as the first cluster center. Then an amount of potential is subtracted from each data point as a function of its distance from the selected cluster center. The data points near the

selected cluster center will have greatly reduced potential, and therefore are unlikely to be selected as the next cluster center. When the potentials of all data points have been revised according to Eq. (28), the data point with the highest remaining potential is selected as the next cluster center:

$$P_{k+1}(i) = P_k(i) - P_k^* e^{-4\| \boldsymbol{x}_i - \boldsymbol{x}_k^* \|^2 / r_\beta^2}, \; i = 1,2,\cdots, N, \tag{28}$$

where $\boldsymbol{x}_k^*$ is the location of the k-th cluster center and P_k^* is its potential value. If the inequality $P_k^* < \omega P_1^*$ is true, these calculations stop, else these calculations are repeated.

The input/output data positioned in the cluster centers are used as the training data set in order to train the three models. The test data is selected every five time-steps among the remaining data that the training data have been eliminated from all acquired data. That is, the optimization data and the test data comprise 80 percents and 20 percents, respectively, of the remaining data. These models are verified by the test data independent of the training data and the optimization data. The three models and the SC selection algorithm for selecting the training data are optimized by a genetic algorithm which was mentioned before.

In case of FSVR, the four parameters (ϵ, λ, σ, μ) are included. As mentioned before, It is reasonable that the data points with high potential calculated by Eq. (27) are more important and weighted more highly than the other neighboring data points when training the FSVR models. Therefore, the potential of the cluster centers calculated by Eq. (27) was used as a fuzzy membership grade in Eq. (7) as follows:

$$\mu_i = 1 - \frac{1}{P_1(i)}, \; i = 1, \cdots, N_c. \tag{29}$$

Ⅴ. *Application to the Welding Residual Stress Prediction*

Initially a finite element model was developed for analyzing welding residual stress. In the developmental process, 150 analysis conditions (welding heat input, pipeline shapes, welding metal strength, and the constraints of the pipeline end parts) were considered as a means of assessing the welding residual stress along two paths in the welding zone (as shown in Fig. 1). But performance computation of the three models (SVR, FSVR and FNN) for predicting the welding residual stress in this thesis was executed in only center path because of complexity of data in inside path. In addition, the ABAQUS code was used to calculate the welding residual stress at 21 locations along each path [7]. In total, 6300 items of welding residual stress data were acquired from the two paths (Fig. 1). Table 1 shows the conditions for analyzing the welding residual stress.

These models can be well trained by using informative data. Input and output training data are expected to have many clusters, and the data at these cluster centers is more informative than neighboring data (refer to Fig. 5.). The cluster centers was selected with an SC scheme and they were used as the training data set. The test data verify the three models, independently of the training data and the optimization data. A genetic algorithm was used to optimize three models while the SC selection algorithm was used for selecting the training data.

The three models were optimized with the training data and the optimization data and then tested with the test data. Tables 2 to 4 show the performance results of the three models, respectively. The relative RMS errors (SVR) of the predicted residual stress are 2.50% for the training data, 2.31% for the optimization data, and 2.80% for the test data. In the FSVR case, 1.34% for the training data, 2.82% for the optimization data, and 2.95% for the test data. In case of FNN,

4.41% for the training data, 2.50% for the optimization data, and 2.72% for the test data, respectively. Note also that the RMS errors of the three models for the test data are similar to the RMS errors for the training data and the optimization data, irrespective of the (restrained and free) constraints and the center path. Therefore, if initially trained and optimized with the training data and the optimization data for a variety of welding conditions and pipeline shapes, the three models can accurately predict the welding residual stress for any other welding condition. In addition, the developed three models can predict welding residual stress with an RMS error level of less than 5% (as shown in Tables 2-4).

Generally, the results of each method confirm that the proposed three models favorably evaluate welding residual stress well. Plus, the performance of FSVR is better than the other methods.

Table 2. Performance of the Proposed SVR Model for Predicting the Welding Residual Stress (Center Path)

Constraint of end section	Data type	RMS error(%)	Relative max error (%)	No. of data	Max. Fitness
Restrained	Training Data	3.3350	33.7051	1261	0.9314
	Optimization Data	2.7770	15.3491	251	
	Test Data	3.8527	24.1245	63	-
Free	Training Data	1.6657	6.2035	1261	0.9833
	Optimization Data	1.8528	7.1262	251	
	Test Data	1.7545	4.1842	63	-

Table 3. Performance of the Proposed FSVR Model for Predicting the Welding Residual Stress (Center Path)

Constraint of end section	Data type	RMS error(%)	Relative max error (%)	No. of data	Max. Fitness
Restrained	Training Data	2.6023	10.3991	1261	0.9521
	Optimization Data	3.1385	13.2690	251	
	Test Data	3.4665	9.3707	63	-
Free	Training Data	0.0844	0.3055	1261	0.9779
	Optimization Data	2.5098	7.5196	251	
	Test Data	2.4246	6.2893	63	-

Table 4. Performance of the Proposed FNN Model for Predicting the Welding Residual Stress (Center Path)

Constraint of end section	Data type	RMS error(%)	Relative max error (%)	No. of data	Max. Fitness
Restrained	Training Data	4.5135	42.1870	1261	0.9131
	Optimization Data	2.9886	11.6960	251	
	Test Data	3.1258	16.9490	63	-
Free	Training Data	4.3153	38.5710	1261	0.9384
	Optimization Data	2.0108	7.2120	251	
	Test Data	2.3117	6.3920	63	-

In order to solve the prospective overfitting problems of artificial intelligence methods and to accomplish the increase of reliability, the different combined models were made and each performance was compared. As shown in Table 5, the model combined with SVR and FSVR provides the best results and is superior to other prediction models.

Table 5. Performance Comparison of the Data-based Models for the Prediction of Residual Stress (Center Path)

Constraint of end section	Methods	RMS error(%)	Relative max error (%)
Restrained	FNN	3.1258	42.1870
	SVR	3.8527	33.7051
	FSVR	3.4665	13.2690
	FNN+SVR+FSVR	2.8477	20.9978
	SVR+FSVR	2.5870	19.7250
	2 out of 3 models	2.8184	28.8881
Free	FNN	2.3117	38.5710
	SVR	1.7545	7.1262
	FSVR	2.4246	7.5196
	FNN+SVR+FSVR	1.7155	14.7229
	SVR+FSVR	1.1314	6.1552
	2 out of 3 models	1.1643	5.7053

Ⅵ. *Conclusions*

Now that the welding residual stress is a major factor to generate Primary Water Stress Corrosion Cracking (PWSCC), it is important to assess the welding residual stress for preventing the PWSCC.

In this thesis, a support vector regression (SVR), a fuzzy support vector regression and a fuzzy neural network (FNN) models have been developed to correctly estimate a residual stress for dissimilar metals welding zones. The three developed models were applied to numerical data obtained by means of FEAs. And because of complexity of data in inside path, implementation of FSVR model for predicting the welding residual stress was executed in only center path. But it is expected that it is possible to accomplish the performance improvement in inside path by selecting proper functions which can assign a fuzzy membership grade to data point.

The three models were trained with the data set prepared for training (the training data), optimized with the optimization data set, and verified with the test data set, which is different from the training data and the optimization data. The developed models can predict welding residual stress with an RMS error level of less than 5%. The RMS errors of the three models for the test data are similar to the RMS error for the training data and the optimization data. Then the models combined with different methods (FSVR, SVR, FNN) have been used to solve the prospective overfitting problems.

Consequently we could confirm that the performance of the model combined with both SVR and FSVR is superior to any other method. Therefore, it is expected that this model can be applied to predict residual stress in dissimilar metals welding zones.

References

[1] M. Mochizuki, "Control of Welding Residual Stress for Ensuring Integrity Against Fatigue and Stress - Corrosion Cracking," Nucl. Eng. Des., Vol. 237, No. 2, pp. 107-123 (2007).

[2] P. Michaleris, J. Dantzig, and D. Tortorelli, "Minimization of Welding Residual Stress and Distortion in Large Structures," Welding J., Vol. 78, No. 11, pp. 361 - 366 (1999).

[3] M.G. Na, J.W. Kim, D.H. Lim, "Prediction of Residual Stress for Dissimilar Metals Welding at NPPs Using Fuzzy Neural Network Models," Nucl. Eng. Tech., Vol. 39, No. 4, pp. 337-348 (2007a).

[4] V. Robin et al., "Modelling of Bimetallic Welds," Proc. Mathematical Modeling of Weld Phenomena 6, Vol. 784, pp. 769-792 (2002).

[5] D. E. Katsareas and A. G. Youtsos, "Residual Stress Prediction in Dissimilar Metal Weld Pipe Joints Using Finite Element Method," Mater. Sci. Forum Vols. 490-491, pp. 53 - 61 (2005).

[6] B. Brickstad and B. L. Josefson, "A Parametric Study of Residual Stresses in Multi-Pass Butt-Welded Stainless Steel Pipes," Int. J. of Press. Ves. & Piping, Vol. 75, No. 1, pp. 11-25 (1998).

[7] Hibbitt, Karlson & Sorensen, Inc., ABAQUS/Standard User's Manual (2001).

[8] M.G. Na, J.W. Kim, D.H. Lim, Y.J. Kang, "Residual Stress Prediction of Dissimilar Metals Welding at NPPs Using Support Vector Regression," Nucl. Eng. Des., Vol. 238, No. 7, pp. 1503-1510 (2008).

[9] A. Kulkarni, V.K. Jayaraman, B.D. Kulkarni, "Control of Chaotic Dynamical Systems Using Support Vector Machines," Physics Letters A, Vol. 317, No. 5, pp. 429-435 (2003).

[10] M.G. Na, and Y.R. Sim, "An Input Feature Selection Method Applied to Fuzzy Neural Networks for Signal Estimation," J. Korean Nucl. Soc., Vol. 33, No. 5, pp.

457-467 (2001).

[11] M.G. Na, J.W. Kim, I.J. Hwang, "Collapse Moment Estimation by Support Vector Machines for Wall-thinned Pipe Bends and Elbows," Nucl. Eng. Des., Vol. 237, Iss. 2, pp. 451-459 (2007b).

[12] P.-F. Pai, W.-C. Hong, "Support Vector Machines with Simulated Annealing Algorithms in Electricity Load Forecasting," Energy Conver. Manage., Vol. 46, No. 17, pp. 2669-2688 (2005).

[13] V. Kecman, "Learning and Soft Computing," MIT Press, Cambridge, Massachusetts (2001).

[14] V. Vapnik, "The Nature of Statistical Learning Theory," Springer, NewYork (1995).

[15] D. P. Bertsekas, "Constrained Optimization and Lagrange Multiplier Methods," Academic Press, New York (1982).

[16] S.L. Chiu, "Fuzzy Model Identification Based on Cluster Estimation," J. Intell. Fuzzy Syst. Vol. 2, No. 3, pp. 267-278 (1994).

[17] T. Takagi and M. Sugeno, “Fuzzy Identification of Systems and Its Applications to Modeling and Control,” IEEE Trans. Systems, Man, Cybern., Vol. 15, No. 1, pp. 116-132 (1985).

[18] I.V. Tetko, D.J. Livingstone, A.I. Luik, “Neural Network Studies. 1. Comparion of Overfitting and Overtraining,” J. Chem. Inf. Comput. Sci., Vol. 35, No. 5, pp. 826-833 (1995).

감사의 글

1년 365일 계속 돌고 있는 실험실 서버의 팬소리...

2년동안 집보다 더 편안했던 이 곳에서 오랜 시간을 보내면서도 이 소리는 신경쓰지 못하였는데.. 이등병 같은 마음으로 논문이란 것은 생각치도 못하며 들어왔던 2006년의 어느 날이 아직도 엊그제 같은데 벌써 2년이라는 세월이 흘러 어느덧 졸업 논문의 마지막을 작성하고 있는 지금 이 순간, 저 팬소리마저도 많은 추억을 담는 NICL 타임캡슐 한 부분에 조용히 자리잡습니다.

“2년 금방이다~” “네가 어떻게 생활하느냐에 따라 2년이 20년 값을 하거나 혹은 2개월 값을 할 수 있다!” 이런 조언을 귀담아 들으며 훗날 후회 하지 않기 위해 나름대로 열심히 지낸다고 지내왔는데 역시 아쉬움만이 머릿속을 가득 채웁니다. 하지만 이 아쉬움이 앞으로 저를 또 다른 곳에서 움직이게 할 원동력임을 확신하며 지금 이 순간도 최선을 다 하려고 합니다. 그리고 다음 모든 분들께 감사의 말씀을 전합니다.

먼저 실수투성이이고 턱없이 부족한 저에게 항상 따뜻한 관심을 가지어 주시고 세상 어느 대학원생과 비교하여도 전혀 손색이 없도록 많은 경험, 전공과 사회생활을 불문한 많은 가르침을 제공해 주신 나만균 교수님께 한없는 감사를 드립니다. 또한 항상 제자가 잘 되기만을 바라시며 걱정해주시고 챙겨주시는 모습과 뜨거운 열정으로 변함없이 학문연구에 매진하시는 모습을 보며 진정으로 사람을 고개 숙일 수 있게 하는 법을 알게 해 주셨습니다. 늘 바쁘신 와중에도 많은 조언을 해 주시는 김숭평 교수님, 사석에서도 신경을 써 주시며 저를 격려하고 자신감을 북돋아 주시는 정운관 교수님, 항상 저를 믿고 맡겨 주시며 후배들로 하여금 귀감이 될 수 있게 좋은 말씀을 해 주시는 이경진 교수님, 항상 안부를 물으시며 관심을 가져주시고 처음으로 교수님이라는 높게만 보였던 장벽을 무너뜨릴 수 있게 해 주신 송종순 교수님 (아직도 사은회때는 잊지 못하고 있습니다.), 비록 제가 직접 수업은 듣지 못했지만 사석에서 실제적인 원

자력에 관한 말씀들 해 주셨던 박원재 교수님, 이기복 교수님께 진심으로 감사의 말씀을 드립니다.

NICL 실험실에서 처음부터 같이 생활을 시작하며 희노애락을 항상 함께 했던 저의 두 원수분들 헌영이형, 인호형 정말 사랑합니다. 형들이 없었다면 어떻게 제가 졸업을 했을지 참 생각만 해도 깝깝한 마음뿐입니다. 두 형들의 이야기로 감사의 글을 써도 한 20장은 나올 듯 한데 뒤에 사람들이 많은 관계로 패스... 그리고 이 시대의 여행꾼 대섭이.. 이번달부터 다 잘되길 바라며 이번에 상병으로 실험실에 들어와 이 곳을 책임질 에이스 성한이 비록 질풍노도의 시기가 지금은 도래해 있지만 넌 정말 최고가 되리라 확신한다. 앞으로도 많은 상담 요청 바란다. 그리고 랩실을 꽉꽉차게 해 준 3학년의 최고들 막내 동수와 심원이.. 니들이 있어 실험실이 보다 깨끗해졌고 활기차졌다. 지금 하는 논문들 잘 쓰고 이렇게 웃으며 랩실 생활하다가 정식으로 입학하길 바란다.

그리고 대학원이라는 매개체를 통해 알게 되고 좋은 말씀을 많이 해 주신 박원서 부장님, 귀성이 형님, 금주 형님, 상준이 형님, 유선이 형님, 철기 형님, 정민이 형님, 종선이 형께 감사드리며 항상 추석, 설날 때 뵈며 교수님과의 이전 추억을 말씀해 주시고 실제적으로 실험실의 궁금한 점을 해결해 주시는 영록이 형님, 동원이 형, 선호 형, 인준이 형, 선미 누나에게 감사하다는 말씀을 드립니다.

항상 학과에서 열심히 일하며 싫으나 좋으나 말을 잘 들어 주며 일을 도와줬던 진행이, 봉주, 희망이, 용진이, 영춘이, 우진이, 강일이, 영빈이, 민준이, 평규, 재환이, 상헌이, 영규, 민수, 경훈이 등 후배들 너무 고맙고 2년간 학과실에서 쫓겨나지 않기 위해 내 말을 잘 들어주고 정말 많은 도움을 줬던 김명희.. 고맙다.

항상 친구라는 행복감을 안겨주며 함께 울고 웃었던 나의 보물들 홍록이, 해진이, 희관이, 민섭이, 희성이, 성식이, 희석이, 재환이, 원욱이, 태식이, 민한이, 영준이, 창

호, 종희, 세영이, 두강이, 순철이, 용철이, 승현이, 민희, 장미 그리고 나영이, 보람이 등등 너무너무 고맙고 잘 되서 맛있는 거 많이 사주마.

교토대의 인연으로 아직까지 많은 도움을 주며 결국은 다시 원자력계에서 함께할 주일이형, 승민이, 영재, 재벌이, 향민이, 연건이, 근영이, 연상이 추가로 태우형까지 한번 르네상스시대의 영웅이 되어 봅시다. 그리고 항상 임반장으로써 부족하지만 열심히 따라주고 개성에서부터 제주도까지 각 기업 전역에 배치되어 있는 항상 고마운 최고의 취준반 멤버들 석중이형, 남순이형, 본구형, 재영이형, 동관이, 일한이, 정아, 은엽아 마지막으로 내가 피날레를 최고로 장식해 줄께요. 기대해 주시길..

마지막으로 한없는 사랑을 주심에도 불구하고 항상 아들들에게 죄인이시라던 부모님.. 이렇게 키워주신 제가 꼭 부모님들께서 물질적인 것이 아니라 정신적으로 항상 뿌듯함과 기쁨을 느끼실 수 있도록 항상 노력하고 발전하는 모습을 보여드리겠습니다. 그리고 사랑하는 동생 동희! 최근까지 많은 안 좋은 일들을 겪으며 많이 힘들겠지만 평상시와 같은 패기로 의기소침하지 말고 힘내서 옛날과 같은 최고의 군인이 되길 바란다. 뒤는 이 형이 책임질테니... 파이팅이다!! 그리고 내 사랑스러운 분신이자 정신적 지주 미영아~ 시베리아 같았던 날 세렝게티 초원으로 바꿔준 이 사랑 너무 고맙고 항상 지루함이 없이 신선함을 주도록 계속 변하는 모습 보여줄게.. 지금처럼 알콩달콩 오래오래 함께 하자꾸나~사랑하고.. 마루도 건강해라..

SVR! FSVR! FNN! 이 놈들 고생많았다. 이젠 헌영이형 인호형 성한이와 함께해라...
항상 NICL 실험실과 원자력공학과의 무궁한 발전을 기원하며.....

2008년 12월

동혁....

저작물 이용 허락서

학 과	원자력공학과	학 번	20077102	과 정	석사
성 명	한글: 임 동 혁 한문 : 林 東 革 영문 : Lim Dong-Hyuk				
주 소	광주광역시 북구 문흥동 천일아파트 2-203				
연락처	E-MAIL : s1552421@naver.com				
논문제목	한글 : 데이터 기반 모델링 방법을 이용한 이종금속 용접부 잔류응력 예측				
	영문 : Residual Stress Prediction in Dissimilar Metals Welding Zones Using Data-based Modeling				

본인이 저작한 위의 저작물에 대하여 다음과 같은 조건아래 조선대학교가 저작물을 이용할 수 있도록 허락하고 동의합니다.

- 다 음 -

1. 저작물의 DB구축 및 인터넷을 포함한 정보통신망에의 공개를 위한 저작물의 복제, 기억장치에의 저장, 전송 등을 허락함
2. 위의 목적을 위하여 필요한 범위 내에서의 편집·형식상의 변경을 허락함. 다만, 저작물의 내용변경은 금지함.
3. 배포·전송된 저작물의 영리적 목적을 위한 복제, 저장, 전송 등은 금지함.
4. 저작물에 대한 이용기간은 5년으로 하고, 기간종료 3개월 이내에 별도의 의사 표시가 없을 경우에는 저작물의 이용기간을 계속 연장함.
5. 해당 저작물의 저작권을 타인에게 양도하거나 또는 출판을 허락을 하였을 경우에는 1개월 이내에 대학에 이를 통보함.
6. 조선대학교는 저작물의 이용허락 이후 해당 저작물로 인하여 발생하는 타인에 의한 권리 침해에 대하여 일체의 법적 책임을 지지 않음
7. 소속대학의 협정기관에 저작물의 제공 및 인터넷 등 정보통신망을 이용한 저작물의 전송·출력을 허락함.

동의여부 : 동의(○) 반대( )

2009년 2월 일

저작자: 임 동 혁 (서명 또는 인)

조선대학교 총장 귀하